TCAD analysis of wide-spectrum waveguides in high-voltage SOI-CMOS

Satadal Dutta[1], Luis Orbe[2], and Jurriaan Schmitz[1].
[1] MESA+ Institute for Nanotechnology, University of Twente, [2] Phoenix B.V., Enschede, The Netherlands.

***Abstract*—A TCAD based analysis is presented on the transmission efficiency η of silicon-on-insulator (SOI) and silicon nitride slab waveguides in a high-voltage standard SOI-CMOS technology, for the spectral range of 480 nm - 1300 nm, and isotropic optical excitation via monolithic Si-based LEDs. The effects of geometry, wavelength and galvanic isolation on η are reported.**

The integration of photonic functionality in CMOS is promising for high-speed data communication, and opto-electronic system-on-chip applications. For most contemporary photonic and/or opto-electronic integrated circuits [1]–[5], CMOS technology is commonly extended with a dedicated waveguide (WG) layer having a low material absorption coefficient (α) and a high refractive index (n) for photonic functionalities [1]. Some industrial CMOS technologies, however, offer built-in thin films suitable as WGs, the most common being the silicon (Si) layer in silicon-on-insulator (SOI) technology [1], [5]–[7]. Recently, a monolithic optocoupler was realized in standard high-voltage SOI CMOS [6], which not only includes an SOI layer as a WG for infrared (IR) light, but also a thin silicon nitride (Si_3N_4) film laid atop the active Si surface, which is a potential WG for visible and IR light [7]–[12]. In addition, the optocoupler comprises an Si LED that exhibits wide-spectrum (400 nm $< \lambda <$ 1300 nm) and isotropic electroluminescence (EL). An Si photodiode (PD) detects light laterally. Such features of the LED, combined with the inherent off-axis alignment of the WGs w.r.t. the LED and the PD, makes the optical transmission efficiency $\eta(\lambda)$ rather difficult to analyze by means other than numerical TCAD simulation.

In this work we first show, using raytracing simulations in Sentaurus, the built-in WG conditions for SOI and Si_3N_4 core layers with SiO_2 cladding, leading to anisotropic transmission. Secondly, via hybrid-mode EM wave simulations, we show how $\eta(\lambda)$ is affected by geometry; namely SOI and/or nitride thickness $t_{SOI/Si3N4}$, link length L, and galvanic isolation in a typical SOI-based optocoupler, with on-chip isotropic optical excitation.

Fig. 1(a) shows the schematic cross-section of the key features of a typical SOI-based optocoupler; a p-n junction Si LED and PD, the shallow trench isolation (STI) of length L, the medium trench isolation (MTI), the buried oxide (BOX), the relatively thin Si_3N_4 layer, and a back-end SiO_2 layer comprising the inter-metal dielectric (IMD). The MTI column, used for galvanic isolation, is typically composed of SiO_2 enclosing a thin Si core. A light ray originating from a point in Si along the p-n junction (EL region of the LED) makes an angle ϕ w.r.t. the positive x-axis ($-90^o < \phi < 90^o$), where ϕ determines the photon trajectory in the optocoupler. Waveguiding via the Si_3N_4 WG requires two necessary conditions. Firstly, $n_{Si}(\lambda) > n_{Si3N4}(\lambda) > n_{SiO2}(\lambda)$, and secondly, $\cos^{-1}(n_{SiO2}(\lambda)/n_{Si}(\lambda)) > \phi > \cos^{-1}(n_{Si3N4}(\lambda)/n_{Si}(\lambda))$. Waveguiding via the SOI WG (without MTI) occurs only if $\phi > -\sin^{-1}(n_{SiO2}(\lambda)/n_{Si}(\lambda))$. If an MTI column is present in the SOI layer, then necessary WG condition is additionally constrained by $\phi > -\cos^{-1}(n_{SiO2}(\lambda)/n_{Si}(\lambda))$. The constraints on ϕ affect the optical transmission, which is captured by extracting the TCAD simulated gain G_{opt} in the PD photo-current I_{PD}, as summarized in Fig. 1(b) at λ = 1100 nm. This choice of λ ensures negligible material absorption in both the WGs. In addition, line-of-sight (LOS) propagation (incurs mainly Fresnel reflection losses) occurs along the x-axis via a small aperture $|\phi| < \delta$ through the STI, with δ depending on L, and t_{STI}.

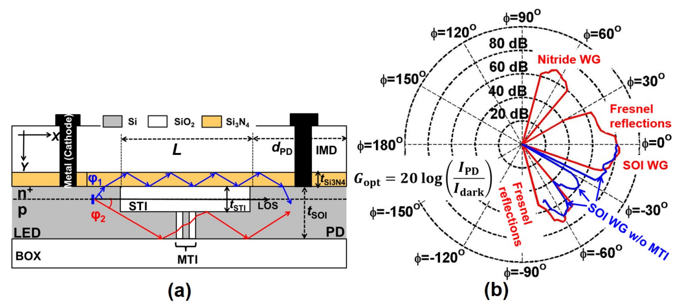

Fig. 1. (a) 2-D schematic cross-section of the SOI-based optocoupler showing relevant parameters and design features, and two example ray-traces when guided via the Si_3N_4 (blue) and the SOI WGs (red). (b) TCAD simulated G_{opt} of the PD versus ϕ at λ = 1100 nm.

Next, the effect of geometry and λ on η for propagation via the SOI WG is studied using 2-D EM wave solver in Sentaurus. Fig. 2(a) shows the structure used as our simulation input deck. The structure is optimized to ensure a low self-absorption of light within the Si LED. A truncated plane-wave (TPW) excitation with mixed TE and TM polarization and a fixed intensity that has spatial divergence, is used to mimic our Si-embedded optical source. The TCAD simulated profiles for optical intensity and the magnetic field intensity $H(x,y)$ are shown for λ = 1100 nm in Figs. 2(b) and (c) respectively, showing optical confinement and guiding via the SOI layer. In Fig. 2(d), we observe that for a fixed t_{SOI} = 1 μm, and any given L, $\eta = P_{out}/P_{in}$ first increases with increasing λ due to a sharp decrease in α_{Si}, reaches a maximum at a certain λ_{peak}, and eventually decreases gradually due to a reduction in the mode-propagation efficiency for longer λ. Further, for a fixed λ, η decreases with increasing L due to absorption. For $\lambda >$ 1150 nm (corresponds to Si band gap

978-1-5090-5323-0/17/$31.00 ©2017 IEEE

of 1.12 eV), η is significantly less sensitive to L, due to negligible absorption at such long λ. In Fig. 2(e), we observe that for a fixed L, $\eta(\lambda)$ increases as t_{SOI} is increased from 1 μm to 2 μm, due to increased mode-propagation efficiency. This also explains the observation that $\eta(\lambda)$ increases till λ = 1300 nm for t_{SOI} = 2 μm; λ_{peak} being shifted beyond 1300 nm. Further, the presence of the MTI, leads to a fixed additional 20 % reduction in η for any L and t_{SOI}, caused by Fresnel reflections at the Si-SiO$_2$ interfaces. The ripples in $\eta(\lambda)$ are likely caused by inter-modal interference.

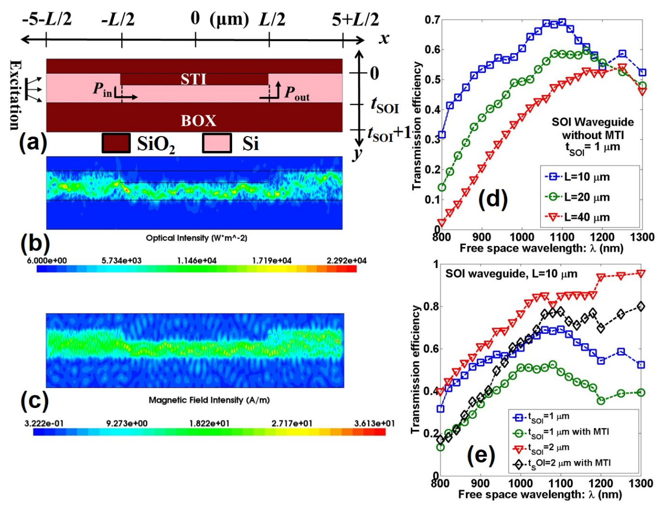

Fig. 2. (a) The SOI WG: The time-averaged and y-integrated input (P_{in}) and output (P_{out}) optical powers are evaluated at x=–0.5 L and x=0.5 L respectively. Convolutional Perfectly Matched Layer (CPML) boundary conditions are assumed in both x and y directions, and t_{STI}=0.4 μm. (b) Optical intensity profile and (c) Magnetic field intensity profile at λ=1100 nm. (d) and (e) Simulated η for indicated values of L and t_{SOI}.

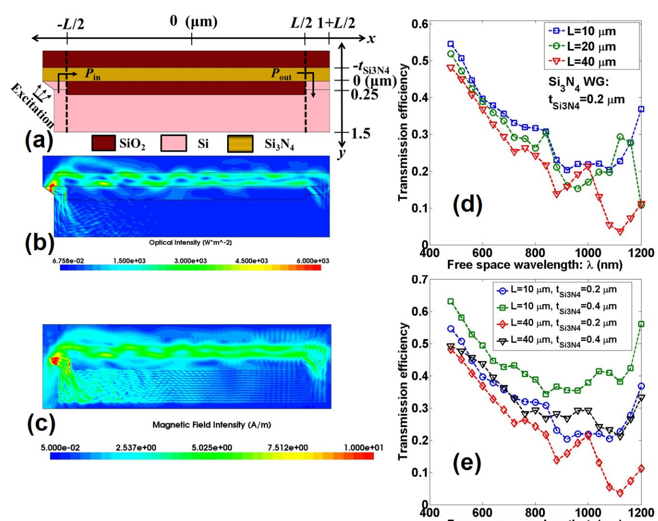

Fig. 3. (a) The Si$_3$N$_4$ WG: Time-averaged and y-integrated input (P_{in}) and output (P_{out}) optical powers are evaluated at x=–0.5 L and x=0.5 L respectively. CPML boundary conditions are assumed for both x and y axes. (b) Optical intensity profile and (c) Magnetic field intensity profile at λ=600 nm. (d) and (e) Simulated η for indicated values of L and t_{Si3N4}.

Fig. 3(a) shows the optimized structure used to simulate the Si$_3$N$_4$ WG. The TPW excitation (constrained by the solver to be placed in vacuum) is given an initial orientation $\phi \approx 62^o$. This mimics our Si-based optical source without violating the aforesaid necessary conditions for waveguiding. Figs. 3(b) and (c) show the intensity profile and $H(x,y)$ respectively at λ = 600 nm, showing out-of-plane guiding. Light is coupled in from the Si LED into Si$_3$N$_4$, and is coupled out from Si$_3$N$_4$ to the Si PD. The Si$_3$N$_4$ core is optically much thinner than the SOI core. In Fig. 3(d), we observe that for a fixed t_{Si3N4} and L, η falls sharply with increasing λ. A slight increase in η is observed for $\lambda \geq$ 1100 nm, which can be explained by an increased edge-coupling to the underlying SOI layer, thereby augmenting P_{out} and hence η for longer λ. Further, $\eta(\lambda)$ shows a much smaller L-dependence (attenuation) than observed in the SOI case, due to the much lower α_{Si3N4}. In real structures, however, a higher attenuation is expected [6] because of roughness in the core-cladding interface (ignored in our simulation). For any L, as t_{Si3N4} is doubled from 0.2 μm to 0.4 μm, a $\sim$ 15 % increase in $\eta(\lambda)$ is observed due to increased mode-propagation efficiency; the increase being more pronounced at longer λ.

The $\eta(\lambda)$ for all the optical paths can be combined to obtain the cumulative weighted $\eta(\lambda)$ over the entire range of ϕ to mimic an isotropic optical source, as shown in Fig. 4(a). Transmission is dominated by the Si$_3$N$_4$ WG for λ <700 nm, and by the SOI WG for λ >700 nm. Our TCAD analysis provides some key guidelines for designers to optimize optical propagation in standard SOI CMOS technology, involving embedded wide-spectrum and isotropic light sources, as highlighted in Fig. 4(b).

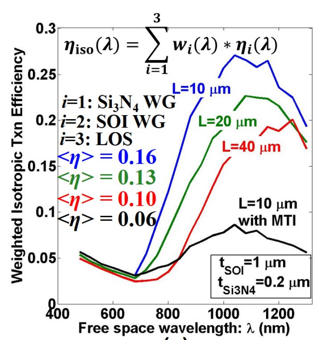

(a)

Summary and future scope

i. For λ > 800 nm, avoiding the MTI in SOI WG improves η, unless galvanic isolation has a higher priority.
ii. A larger SOI WG core thickness (= $t_{SOI} - t_{STI}$) improves η, but increases inter-modal interference.
iii. For λ < 800 nm, guiding occurs via Si$_3$N$_4$, which must be present between high index Si and low index SiO$_2$. Optical excitation close to the Si-Si$_3$N$_4$ interface reduces absorption losses in Si.
iv. The $\eta(\lambda)$ can further be multiplied with the normalized spectral irradiance of any broadband light-emitter to obtain an emission-specific spectral transmission coefficient.

(b)

Fig. 4. (a) ϕ-weighted cumulative transmission efficiencies for indicated geometrical parameters assuming isotropic EL combining the three optical paths: Si$_3$N$_4$ WG, SOI WG, and LOS. The weights $w_i(\lambda)$ are calculated using the allowed range of ϕ for each path, such that $\Sigma w_i(\lambda)$ = 1. The mean spectral efficiency $< \eta >$ is indicated for each case. (b) Summary of the key take-away messages of our work and its potential scope of application.

References

[1] C. Sun et al., Nature, vol. 528, pp. 534-538, 2015.
[2] M. du Plessis et al., IEEE J. Sel. Topics Quantum Electron., vol. 8, no. 6, pp. 1412-1419, 2002.
[3] B. Huang et al., Opt. Commun., vol. 284, no. 16-17, pp. 3924-3927, 2011.
[4] A. Khanmohammadi et al., Proc. 45th ESSDERC, pp. 138-141, 2015.
[5] N. Rouger et al., Proc. 28th ISPSD, pp. 427-430, 2016.
[6] S. Dutta et al., Opt. Express, vol. 25, no.4, pp. 5440-5456, 2017.
[7] R. Baets et al., in proc. OFC 2016, p. Th3J.1.
[8] A.Z. Subramanian et al., IEEE Photonics J., vol. 5, no. 6, 2013.
[9] M. Melchiorri et al., Appl. Phys. Lett., vol. 86, 121111, 2005.
[10] H. Yamada, Piers Online, vol. 6, no. 2, 2010.
[11] G. Li et al, Opt. Express, vol. 20, no. 11, pp. 12035-12039, 2012.
[12] F. Grillot et al., J. Lightwave Tech., vol. 24, no. 2, 2006.